NASA TECHNICAL NOTE

NASA TN D-5569

c. 1

NASA TN D-5569

ALPHA-GAMMA ANGULAR CORRELATIONS IN THE REACTION TIN-120 $(\alpha, \alpha' \gamma_{1.18 MeV})$

by Regis F. Leonard, William M. Stewart, and Norton Baron

Lewis Research Center
Cleveland, Ohio

NATIONAL AERONAUTICS AND SPACE ADMINISTRATION • WASHINGTON, D. C. • DECEMBER 1969

1. Report No. NASA TN D-5569	2. Government Accession No.	3. Recipient's Catalog No.
4. Title and Subtitle ALPHA-GAMMA ANGULAR CORRELATIONS IN THE REACTION TIN-120 (α, $\alpha'\gamma_{1.18MeV}$)		5. Report Date December 1969 6. Performing Organization Code
7. Author(s) Regis F. Leonard, William M. Stewart, and Norton Baron		8. Performing Organization Report No. E-5181
9. Performing Organization Name and Address Lewis Research Center National Aeronautics and Space Administration Cleveland, Ohio 44135		10. Work Unit No. 129-02 11. Contract or Grant No.
12. Sponsoring Agency Name and Address National Aeronautics and Space Administration Washington, D.C. 20546		13. Type of Report and Period Covered Technical Note 14. Sponsoring Agency Code
15. Supplementary Notes		

16. Abstract

The angular correlation between inelastically scattered 42-MeV alpha particles and gamma rays emitted in the subsequent nuclear decay has been studied for the 1.18 MeV (2^+) state of tin-120. The symmetry angle and the magnitude of the anisotropy of the gamma distribution have been measured for alpha-scattering angles between 15^o and 60^o. The results are compared with the distorted-wave predictions and with the adiabatic model. The observed symmetry angles in no way aid in removing the optical model ambiguities that exist for 42-MeV alpha particle scattering on tin.

17. Key Words (Suggested by Author(s)) $^{120}Sn(\alpha, \alpha'\gamma_{1.18MeV})$ Alpha-gamma correlations		18. Distribution Statement Unclassified - unlimited	
19. Security Classif. (of this report) Unclassified	20. Security Classif. (of this page) Unclassified	21. No. of Pages 20	22. Price* $3.00

*For sale by the Clearinghouse for Federal Scientific and Technical Information
Springfield, Virginia 22151

ALPHA-GAMMA ANGULAR CORRELATIONS IN THE REACTION TIN-120 $(\alpha, \alpha' \gamma_{1.18 MeV})$

by Regis F. Leonard, William M. Stewart, and Norton Baron

Lewis Research Center

SUMMARY

The angular correlation between inelastically scattered alpha particles and gamma rays emitted in the subsequent nuclear decay has been measured for scattering with excitation of the 1.176-MeV state of tin-120. The symmetry angle of the gamma distribution has been measured for center-of-mass scattering angles between 15^o and 60^o. The experimentally observed symmetry angles were close to the adiabatic predictions over the range of alpha-particle scattering angles θ_α studied, except for a rapid rotation at $\theta_\alpha = 24^o$, and a possible one at $\theta_\alpha = 15^o$. The results are compared with the predictions of a distorted-wave Born calculation performed using a wide range of optical model potentials, none of which predicted the rotations found in the data.

INTRODUCTION

The inelastic scattering of medium energy alpha particles excites predominately collective states, and in particular, the first 2^+ state of even-even nuclei. Several theories can predict the cross section for the scattering of alpha particles for nuclei in the mass region of tin with fairly good results. The angular correlation, however, is more sensitive to the details of the calculation because it depends on the phases of the transition amplitudes, while the cross section depends only on the magnitudes.

Previously the differential cross section for the elastic and first 2^+ state of tin-120 (^{120}Sn) have been measured (ref. 1). Good four-parameter optical model fits were obtained for the elastic scattering data. The optical model analysis of the elastic tin data showed considerable ambiguity in the optical model parameters obtained, as is common in the scattering of medium energy alpha particles. It has been shown (ref. 2), that in the mass region of tin the ambiguities are due to a surface reflection as opposed to the volume absorbtion found in the lighter nuclei (ref. 3).

The distorted-wave Born approximation (DWBA) calculation for the inelastic scattering to the first 2^+ state of ^{120}Sn were of no help in removing the optical model ambiguities because the DWBA fits to the inelastic data were essentially equivalent for all sets of optical model parameters.

The measurement of the angular correlation between the inelastically scattered alpha particle and the de-excitation gamma ray from the 1.176-MeV state was undertaken in hopes of obtaining useful data complimenting the scattering cross sections. It was hoped that the DWBA predictions of the correlation pattern would allow us to obtain a unique set of optical model parameters. If this could be done, then, in the framework of the direct reaction theory, we would have a better understanding of the alpha scattering reaction mechanism.

SYMBOLS

A	magnitude of isotropic component of alpha-gamma correlation function
a_i	diffuseness of form factor for imaginary part of optical potential
a_o	diffuseness of form factor for real part of optical potential
B	magnitude of anisotropic component of alpha-gamma correlation function
F_{LM}	reduced transition amplitude
$\langle j_1 m_1 j_2 m_2 / JM \rangle$	Clebsh-Gordan coefficient for addition of angular momentum $j_1 m_1$ and $j_2 m_2$ to obtain resultant JM
k	wave number of incident alpha particle
L	orbital angular momentum
N	number of data points used in optical model search
n_i	number of parameters used in optical model search
R_o	nuclear radius constant
r	simiclassical interaction radius
r_i	radius of form factor for imaginary part of optical model potential
r_o	radius of form factor for real part of optical model potential
V	strength of real part of nuclear optical potential
V(r)	nuclear optical potential

W	strength of imaginary part of nuclear optical potential
$W(\theta_\gamma)$	correlation pattern in reaction plane
$Y_l^m(\theta, \varphi)$	spherical harmonic of order l, m
θ_o	symmetry angle of alpha-gamma correlation function
θ_α	scattering angle for alpha particles in center of mass system
θ_γ	angle of emission of gamma-ray relative to incident beam direction
$d\sigma/d\Omega$	differential cross section
φ	azimuthal angle for coordinate system
χ^2	measure of statistical goodness of fit

EXPERIMENTAL ARRANGEMENT

Beam Handling

The experiment was performed using the 42.0±0.2-MeV alpha particle beam of the NASA 152-centimeter cyclotron. A schematic diagram of the scattering system is shown in figure 1. The system was designed to reduce the gamma-ray background to a minimum in the target area. The cyclotron beam is focused by a quadrupole magnet on slit S_1, set at a width of 1 millimeter. Slit S_1 acts as a source slit for the 60^o magnet. The magnet's principal purpose in this experiment was simply to bend the beam into the scattering chamber and away from the neutrons coming down the original beam line. Slit S_2, which was located 56 centimeters from the exit of the magnet, was ordinarily set to a width of about 1 millimeter. Slit S_3, located 159 centimeters from the exit of the magnet and set at a width of 1.5 millimeters, defined the direction of the beam incident on the target. Slit S_3 was 327 centimeters from the target and was located inside the concrete shielding wall, with 90 centimeters of lead shielding placed behind it to reduce unwanted slit scattering and gamma rays in the target area. The Faraday cup was removed from the target room by passing the beam duct through a hole in the wall 300 centimeters from the target. The Faraday cup was located 137 centimeters in the ground behind the target room wall. The unwanted gamma-ray background was very low for the system and the gamma-ray detector count rate showed only a few percent increase for the beam passing through the scattering chamber with no target in the beam.

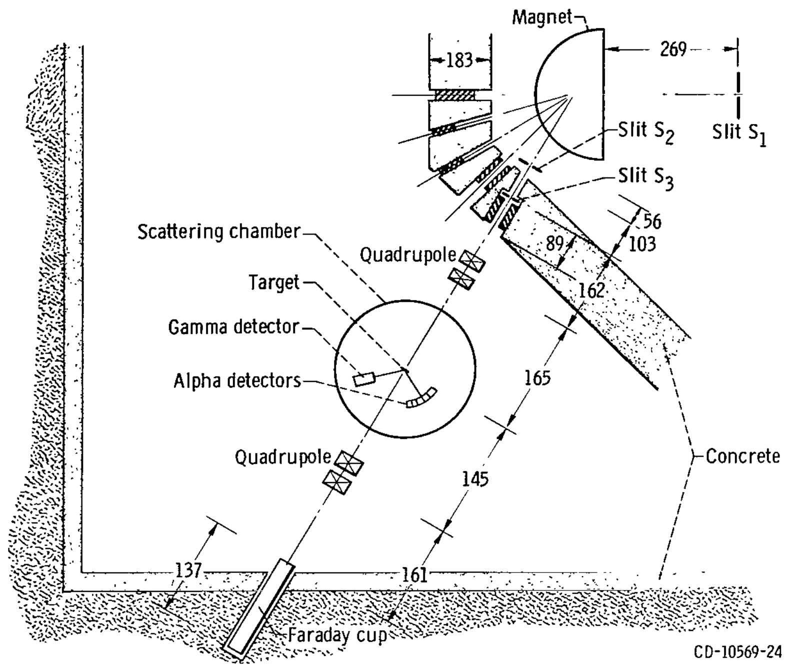

Figure 1. - Schematic diagram of scattering system. (All dimensions are in cm.)

Detectors

The charged particles were detected in lithium-drifted solid-state detectors, which were produced at Lewis (ref. 4). Ten detectors were employed simultaneously in a mount previously described (ref. 4). The detectors were separated by 4° and had a full angular resolution of 1° for angles greater than 25°, and 0.25° for smaller angles. The mean alpha scattering angle was known with an accuracy of $\pm 0.05^{\circ}$.

Gamma rays were detected by a 7.62- by 7.62-centimeter sodium iodide (Tl) crystal. The front face of the detector was 12.7 centimeters from the target and the full angle subtended by the detector was about 35°.

Electronics

The electronics used have been described in detail in reference 5. They were for the most part commercially available units except for the 16-channel router, which was designed and built at this laboratory by T. E. Fessler. A schematic diagram of the electronics is shown in figure 2. The signals from the individual preamplifiers were mixed in the router and proper logic performed so that they were routed to one of the sixteen 256 channel subgroups of the analyzer memory. The coincidence arrangement was a

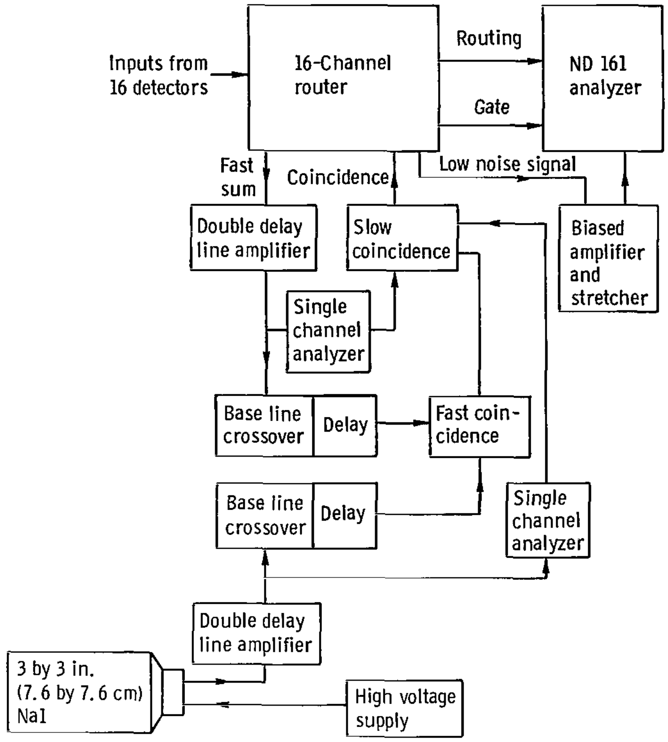

Figure 2. - Multidetector coincidence arrangement using 16-channel router.

typical fast-slow coincidence setup, using crossover pickoff for the fast timing signal. The gamma single-channel analyzer was set so that there was energy selection on the coincidence requirements. The resolving time of the fast-coincidence circuit was run at 50 nanoseconds, which is approximately half of the cyclotron duty cycle.

EXPERIMENTAL DATA

The raw data for this experiment consisted of the energy spectra of the scattered alpha particles taken in coincidence with the 1.176-MeV gamma ray from the de-excitation of the first 2^+ state of ^{120}Sn. Typical results are shown in figure 3. The number of counts in each peak of the spectrum was determined by summing the appropriate analyzer channels and subtracting the accidental coincidences. These random counts were determined by using the fact that all elastically scattered alpha particles in the coincidence spectrum are accidental. The number of elastic counts in the coincidence spectrum multiplied by the ratio of the inelastic (first 2^+ state) cross section to the elastic cross section gave one the number of random counts in each coincidence spectrum. Before and

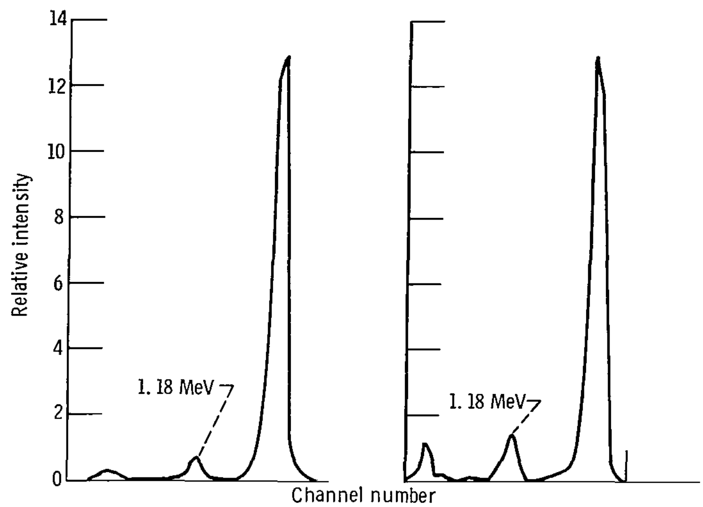

(a) Singles spectrum. (b) Coincidence spectrum; gamma-ray emission angle, 105°.

Figure 3. - Typical spectra of alpha particles scattered from the reaction tin-120 (α, α'). Alpha-particle scattering angle, 36°.

after each coincidence run a singles run was made to check the ratio of the inelastic to the elastic cross section. The average of the before and after singles runs taken over the range of the 10 gamma angles was used in the random count correction.

The experimental data were taken over angular ranges of $15^o \leq \theta_\alpha \leq 60^o$ and $45^o \leq \theta_\gamma \leq 145^o$. The gamma angular range was covered in 10^o steps and the alpha-particle range in 2^o steps. The coincidence runs were normalized relative to a monitor alpha detector located at approximately 30^o below the beam line in the forward direction. Experimental difficulties arose chiefly from two sources. The first is the relatively small fraction of the total reaction cross section (approximately 2 barns), which may be attributed to inelastic scattering. This results in a large target-induced gamma-ray background. This is evident in that no photopeak corresponding to the 1.176-MeV gamma was visible in the gamma-ray spectrum shown in figure 4. As a result the true-to-chance ratio for the currents used (25 nA at angles larger than 25^o) averaged a rather poor one to six. Second, as seen in figure 5, at forward angles the elastic cross section is several orders of magnitude larger than the inelastic cross section. Consequently, it became extremely difficult to resolve the inelastically scattered alpha from the low-energy tail of the elastically scattered ones. As a result it was impossible to obtain correlation data at angles smaller than 15^o.

For the sequence of spins ($0^+ \rightarrow 2^+ \rightarrow 0^+$) the form of the correlation pattern $W(\theta_\gamma)$ in the reaction plane for a fixed alpha scattering angle is (ref. 6)

$$W(\theta_\gamma) = A + B \sin^2 2(\theta_\gamma - \theta_0) \quad (1)$$

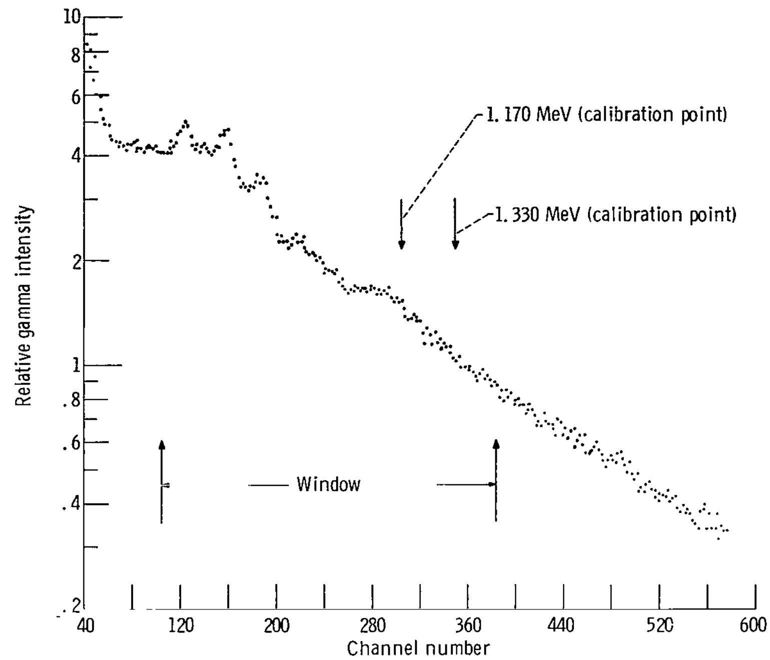

Figure 4. - Gamma-ray singles spectrum from reaction tin-120 (α,γ).

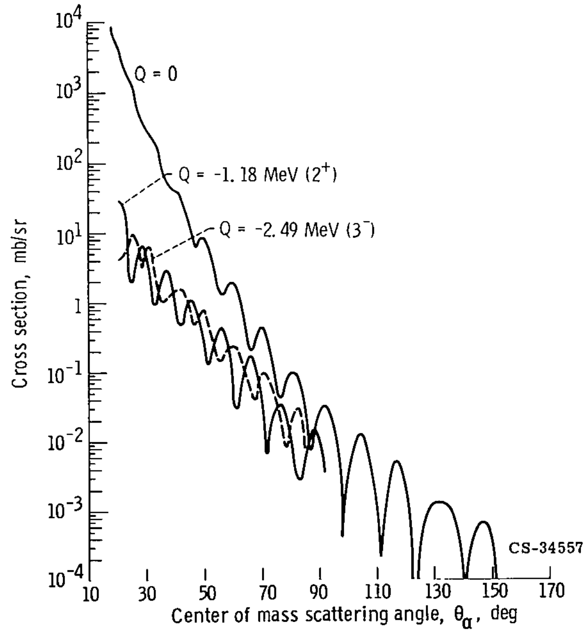

Figure 5. - Tin-120 differential cross section.

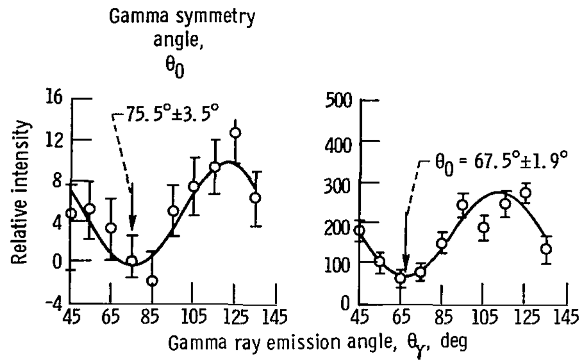

(a) Laboratory alpha-particle scattering angle, 19°.
(b) Laboratory alpha particle scattering angle, 28°.

Figure 6. - Typical correlation patterns with least square fits to function $W(\theta) = A + B \sin^2 2(\theta_\gamma - \theta_0)$.

The coordinate system used is spherical with the polar axis along the incident beam direction and the azimuthal angle measured from the plane determined by the scattered alpha particle. All gamma rays measured in this work were for the azimuthal angle $\varphi_\gamma = \pi$. The measured correlation patterns were fit by the functional form of equation (1) using a linear least squares fitting program, as described in reference 7. Typical experimental patterns and fits are shown in figure 6. The parameters determined from these measurements are the symmetry angle θ_0 and the A/B ratio. The A/B ratio was corrected for the effects of the finite geometry of the gamma detector using the

TABLE I. - TIN-120 $(\alpha, \alpha'\gamma)$ EXPERIMENTAL RESULTS CORRECTED FOR FINITE GEOMETRY

Alpha center-of-mass scattering angle, θ_α, cm, deg	Gamma-ray symmetry angle, θ_0, deg	Ratio of isotropic to anisotropic component, A/B	Alpha center-of-mass scattering angle, θ_α, cm, deg	Gamma-ray symmetry angle, θ_0, deg	Ratio of isotropic to anisotropic component, A/B
15.49	79.23±32.61	0±2.986	35.07	58.16±4.97	0.022±0.190
16.53	55.10±6.65	0.098±0.241	37.12	62.03±2.36	0.070±0.078
17.56	61.08±7.17	0±0.308	39.18	67.78±2.88	0.001±0.009
19.26	75.50±3.53	0±0.100	41.23	67.44±3.64	0±0.118
20.65	72.65±5.98	0±0.187	43.28	68.86±7.90	0±0.311
21.68	78.17±5.50	0±0.157	45.33	44.78±11.41	0.358±0.423
23.75	15.96±28.70	3.042±8.799	47.37	66.53±7.15	0.209±0.266
24.78	54.97±6.36	0.084±0.185	49.42	15.71±65.67	1.158±6.930
25.81	60.78±7.03	0.292±0.248	51.46	51.67±36.57	0±2.754
26.84	63.13±3.14	0.081±0.115	53.51	60.14±8.60	0±0.441
28.90	67.46±1.95	0.219±0.008	55.55	67.76±8.61	0±0.366
30.96	64.37±3.23	0.580±0.188	59.62	62.11±6.98	0±0.515
33.01	67.31±5.17	0.182±0.207			

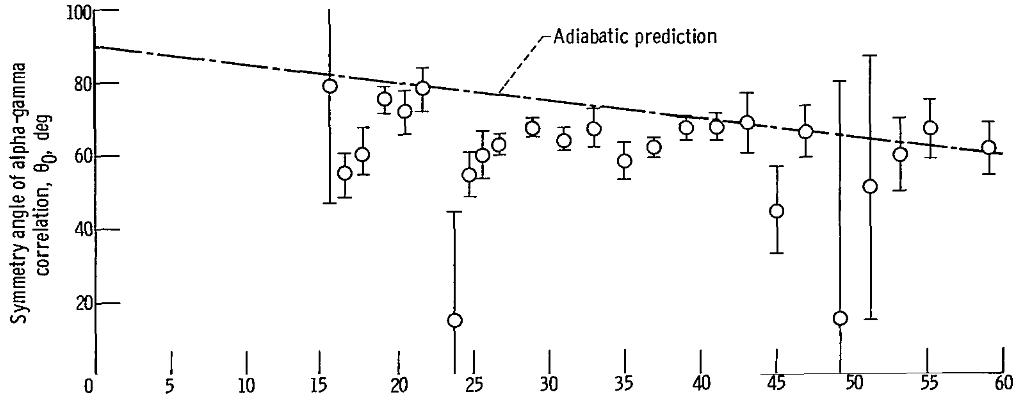

Figure 7. - Gamma-ray symmetry angle for reaction $^{120}Sn(\alpha, \alpha'\gamma)$.

method of Rose (ref. 8). The parameters obtained are listed in table I, and the symmetry angle data are shown graphically in figure 7.

The A/B ratios are not shown graphically since in most cases the errors considerably exceed the value of the ratio. This is due largely to the poor statistics that could be obtained. The effect is more drastic in the A/B ratio than in the symmetry angle since it is the ratio of two measured quantities, each of which suffers independently from the poor statistical accuracy.

DISCUSSION OF THEORY

Several theories can predict the angular correlation as well as the inelastic scattering cross sections. Two of these theories are the adiabatic approximation (refs. 9 and 10), and the plane-wave Born approximation (refs. 11 and 12). The symmetry angle in the first case follows the adiabatic direction of recoil of the target nucleus. In the plane-wave Born approximation the symmetry angle follows the nonadiabatic recoil direction of the target nucleus. For angles greater than 20°, these two theories predict essentially the same symmetry angle as shown in figure 8.

It is well known, however, from studies of other nuclear reactions that neither the plane-wave Born approximation nor the adiabatic approximation is very realistic. A more satisfactory approach for most (ref. 13) nuclear reactions is the use of the distorted-wave Born approximation (DWBA) in which the incident and exit waves are described asymptotically, not as plane waves, but as waves which have been distorted to fit the elastic scattering from the same nucleus.

DWBA calculations have been particularly successful in describing nuclear reactions involving medium and heavy weight nuclei, where the statistical assumptions of the optical

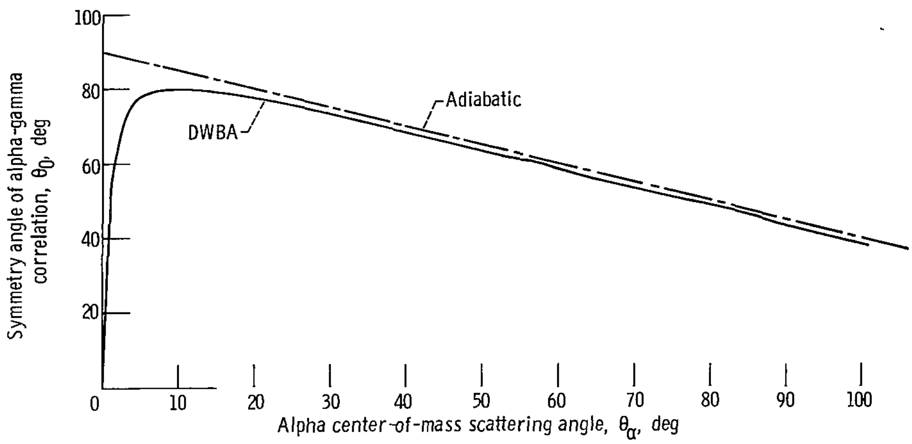

Figure 8. - Symmetry angle as predicted by adiabatic approximation and plane-wave Born approximation.

model are best justified. One encounters a problem, however, in that the optical potential necessary to generate the distorted waves is not uniquely defined by the elastic scattering of strongly absorbed particles such as alphas and deuterons. The reasons for these ambiguities have been discussed (ref. 3). For the alpha energy involved here and for nuclei as heavy as tin, it appears that the ambiguities arise because the scattering is due mainly to reflections at the nuclear surface (ref. 2). Consequently any two nuclear potentials that are the same at large radii will produce the same scattering. In the present work a Woods-Saxon nuclear potential of the form

$$V(r) = -(V + iW)\left[1 + \exp\left(\frac{r - r_o A^{1/3}}{a_o}\right)\right]^{-1} \tag{2}$$

was used. For this particular potential the requirement that the outer edges of the potentials be similar takes the form (ref. 2)

$$\left.\begin{aligned} V \exp\left(\frac{r_o A^{1/3}}{a_o}\right) &= \text{Constant} \\ W \exp\left(\frac{r_o A^{1/3}}{a_o}\right) &= \text{Constant} \\ a_o &= \text{Constant} \end{aligned}\right\} \tag{3}$$

In addition to the four parameters indicated in equation (2), it is possible to introduce two others. This is accomplished by allowing the real and imaginary parts of the nuclear potential to have different radii and diffusenesses. As a rule, this does not lead to any great improvement in describing elastic and inelastic scattering of alpha particles, although some improvement has been reported in scattering from ^{58}Ni (ref. 14). No data of course are available on whether any improvement is obtained by using a six- rather than four-parameter potential to describe angular correlations.

It is fairly well established that DWBA calculations of inelastic scattering cross sections are of little value in determining whether one optical model potential is more valid than another (ref. 2). It was believed then that a comparison of angular correlation data with the predictions of a DWBA calculation would indicate that some potentials are better descriptions of the scattering than others. The basis for this belief is the form of the expression for the correlation pattern in the geometry used here (ref. 15)

$$W(\theta\gamma) = \sum_{\substack{m_l m_l' \\ l\,m}} F^*_{Lm_l} F_{Lm_l'} \langle 2l_m, Lm_l' | Lm_l \rangle \langle L1, L-1 | 2l0 \rangle Y^m_{2l}(\theta_\gamma, \pi) \tag{4}$$

as compared with that for the cross section

$$\frac{d\sigma}{d\Omega} = \sum_m \frac{|F_{Lm}|^2}{2L + 1} \tag{5}$$

where the F_{LM}'s are transition amplitudes as defined in reference 16. It is clear that the first expression is sensitive to the phases of the transition amplitudes F_{LM} while the cross section involves only the squares of their absolute values.

DISCUSSION OF DATA AND CALCULATIONS

The elastic and inelastic cross sections for scattering of 42-MeV alpha particles from ^{120}Sn have been discussed in detail in reference 1. The cross sections exhibit a typical diffraction-type structure and obey the Blair phase rule.

The angular correlation data are distinguished by the presence of a rapid reverse rotation of the symmetry angle near an alpha scattering angle of 24° and a possible rapid rotation near 15°. Except for these two regions, it appears that there are no large departures from the adiabatic prediction. This behavior is similar to that observed in gamma correlation studies on carbon-12, magnesium-24, and nickel-58 (refs. 5, 7, and 17). In the carbon-12 nuclei it appears that the rapid rotations occurred at minima in the inelastic cross section for alpha scattering angles up to θ_{max} and that the symmetry angle remained relatively close to the adiabatic prediction for alpha scattering angles larger than θ_{max}. Since these minima are predicted fairly accurately by Blair's diffraction model (ref. 9), this means in each nucleus θ_{max} should correspond to approximately the same value of the scattering argument used in that theory, namely, $kR_o \sin \theta/2$.

It was believed that magnesium-24 also followed this pattern with its last large rotation at 45^o. Recent data have shown that the last large rotation is at approximately 20^o, which corresponds to the rapid rotation at smaller alpha scattering angle in the other nuclei studied. The comparison of the rapid rotations in the symmetry angles is shown in table II.

The A/B ratios, measured with the accuracy attainable here contain very little information. At only one angle, $\theta_\alpha = 30.96^o$, was it possible to say for certain that the correlation pattern had a nonzero isotropic component, in conflict with adiabatic and plane-wave predictions (refs. 11 and 12).

Optical model calculations using the computer program SCAT 4 (ref. 18) give good agreement with the elastic cross-section data, however, ambiguities of the type discussed earlier were present. Eight equally good four-parameter potentials are listed in table II, and the results of calculations with three of these are shown in figure 9.

In figure 10 calculated inelastic cross sections are compared with the experimental values. The potentials used are the three optical model potentials whose elastic fits are shown in figure 9. The inelastic calculations were done using the direct-reaction calculation (DRC) program of Gibbs et al. (ref. 16). The agreement with the data is good over the whole range of optical model potentials, demonstrating again that the inelastic cross sections in no way aid in removing optical model ambiguities.

TABLE II. - COMPARISON OF ROTATIONS IN SYMMETRY ANGLE DATA

Nucleus	Last Rotation in symmetry angle, deg	Scattering angle argument, $kR_o \sin \theta/2$	Second rotation in symmetry angle, deg	Scattering angle argument, $kR_o \sin \theta/2$
Carbon-12	47	0.914 kR_o	27	0.534 kR_o
Magnesium-24	20	0.501 kR_o	--	---------
Nickel-58	28	0.937 kR_o	20	0.670 kR_o
Tin-120	24	1.01 kR_o	16	0.672 kR_o

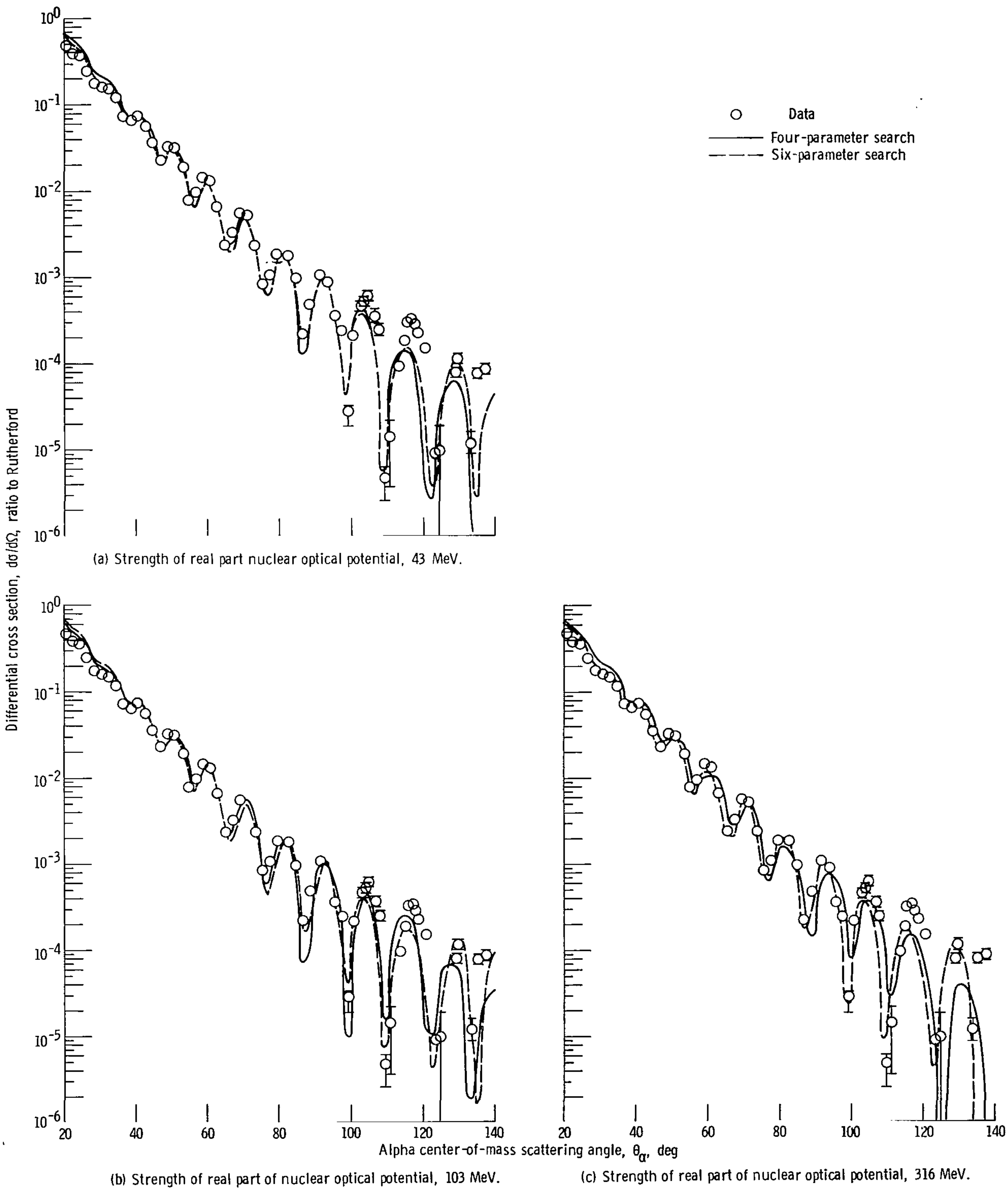

(a) Strength of real part nuclear optical potential, 43 MeV.

(b) Strength of real part of nuclear optical potential, 103 MeV.

(c) Strength of real part of nuclear optical potential, 316 MeV.

Figure 9. - Elastic angular distribution of alpha particles scattered from tin-120.

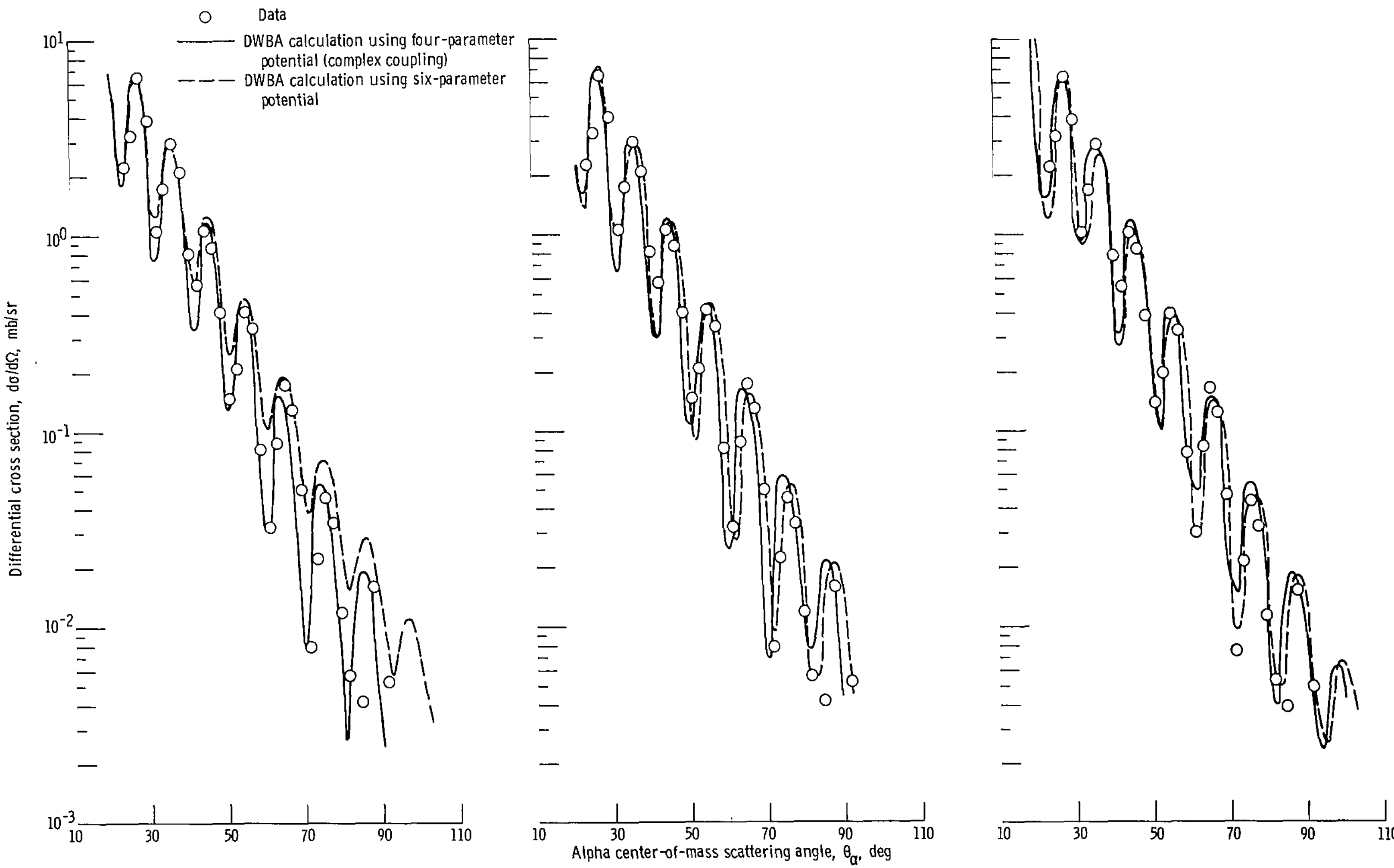

(a) Strength of real part of nuclear optical potential, 43.4 MeV.

(b) Strength of real part of nuclear optical potential, 103 MeV.

(c) Strength of real part of nuclear optical potential, 316 MeV.

Figure 10. - Differential cross sections for inelastic scattering of 42-MeV alpha particles from tin-120.

In figure 11 the calculated symmetry angles are compared with the experimental data. The transition amplitudes are calculated by the DRC program and the symmetry angle is calculated using equation (4). All eight of the potentials predict nearly identical correlation patterns for alpha scattering angles larger than 10°. Three of the potentials ($V = 87.7$, 103, and 117 MeV) predict a reverse rotation of the symmetry angle near $\theta_{\alpha} = 5^{\circ}$ while the others predict a rapid forward rotation in that region. Beyond 10° all the potentials tested predict that the symmetry angle should stay relatively close to the adiabatic or plane-wave prediction, shown as the solid straight line in figure 7. There are small excursions with the calculation crossing the adiabatic line with a small positive slope at angles that correspond to maxima in the inelastic distribution and with a large negative slope at angles that correspond to minima in the inelastic cross section. Unfortunately none of the potentials could be said to yield good fits since none of them were able to predict the rapid rotation, which is seen experimentally near 24°, nor the one which it seems likely occurs at 16°.

As suggested in the section DISCUSSION OF THEORY, further attempts to fit the correlation data were made, using a six- rather than four-parameter optical model. Six-parameter potentials were found by using the four-parameter potentials listed in table III as starting points and allowing SCAT 4 to optimize all six parameters. The potentials which resulted from this procedure are listed with the four-parameter starting potentials in table III. In every case the optimum imaginary radius was larger than the real radius while the best value for the imaginary diffuseness was smaller than that for the real diffuseness. These parameters were used as input for DWBA calculation using a slight modification of the DRC program, in which a six-parameter potential is used in the entrance and exit channels, and the form factor which produces the inelastic scattering is allowed to be complex and is generated by deforming both the real and imaginary parts of the optical potential. In the present case it seems clear that no great improvement should be expected in the fits to the cross sections; however, there is room for considerable improvement in the fits to the correlation data. The results obtained using three of the six-parameter potentials are shown as the dashed lines in figures 9 to 11. It is clear that there has been a slight improvement in the inelastic fits. In particular, at large angles the peaks in the cross sections have been shifted to slightly larger angles, resulting in a somewhat better fit. The correlation patterns, however, are essentially identical in every case to those obtained using a four-parameter potential to describe the scattering.

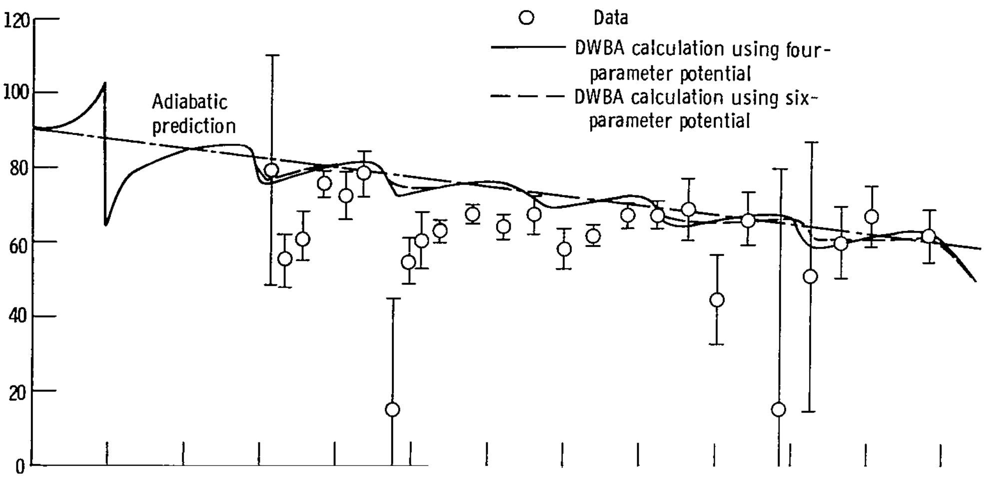

(a) Strength of real part of nuclear optical potential, 43 MeV.

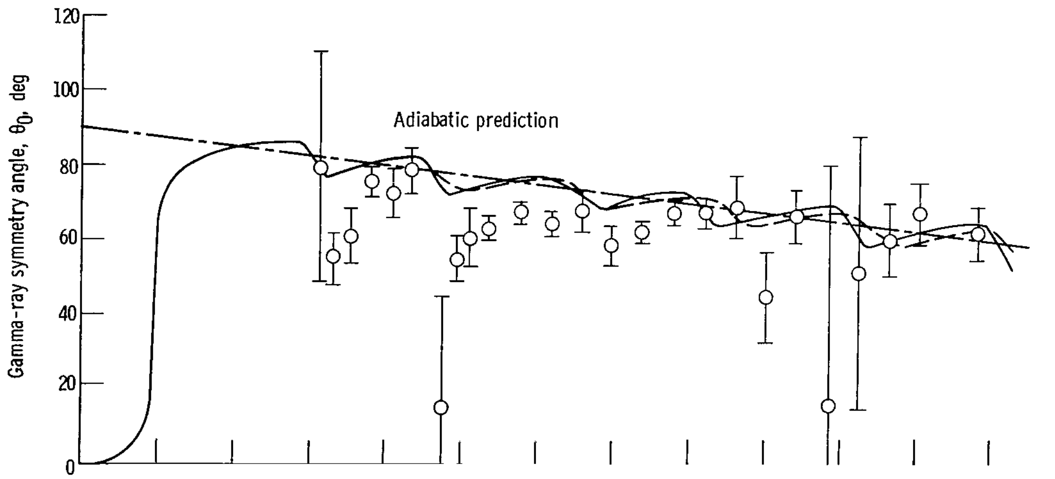

(b) Strength of real part of nuclear optical potential, 103 MeV.

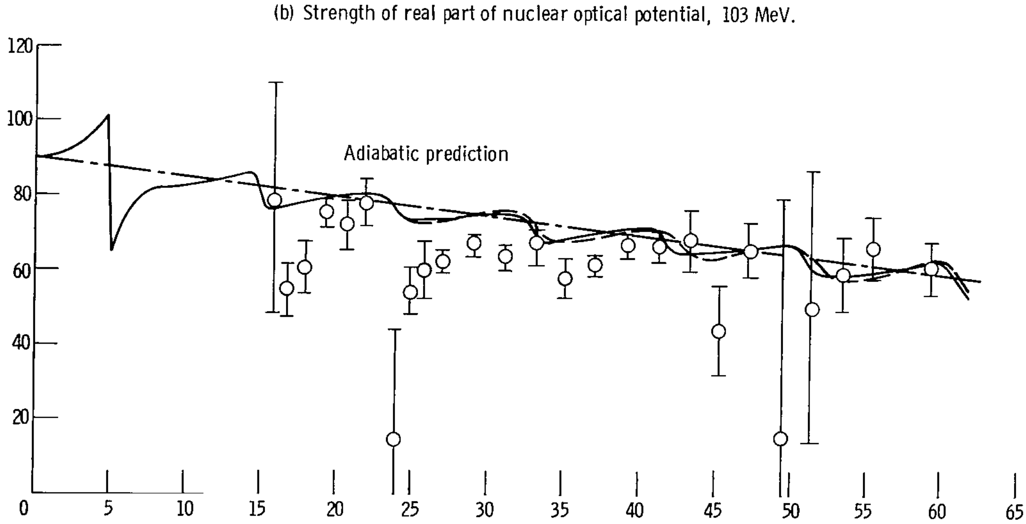

(c) Strength of real part of nuclear optical potential, 316 MeV.

Figure 11. - Gamma-ray symmetry angles for the reaction tin-120 ($\alpha,\alpha'\gamma$).

TABLE III. - TIN-120 OPTICAL MODEL SEARCHES

Real strength, V, MeV	Radius of real potential, r_o, fm	Diffuseness of real potential, a_o, fm	Imaginary strength, W, MeV	Radius of imaginary potential, r_i, fm	Diffuseness of imaginary potential, a_i, fm	Goodness of parameter fit, $\chi^2/N - n_i$	Number of search parameters, n_i
43.40	1.50	0.710	22.50	----	-----	7.28	4
42.84	1.47	.724	22.80	1.52	0.605	5.04	6
58.00	1.46	0.712	28.00	----	-----	7.28	4
59.34	1.42	.716	28.38	1.48	0.609	5.15	6
52.00	1.48	0.703	24.90	----	-----	7.28	4
51.67	1.44	.722	25.06	1.50	0.608	5.31	6
66.10	1.44	0.710	31.10	----	-----	7.28	4
66.38	1.41	.716	31.19	1.46	0.608	5.06	6
87.70	1.40	0.708	38.50	----	-----	7.28	4
87.68	1.37	.714	38.60	1.43	0.615	5.12	6
103.00	1.38	0.705	42.60	----	-----	7.28	4
103.14	1.34	.716	42.83	1.41	0.619	5.10	6
117.00	1.36	0.707	48.00	----	-----	7.56	4
116.93	1.32	.716	48.03	1.40	0.615	5.10	6
316.00	1.19	0.710	145.00	----	-----	29.20	4
316.28	1.18	.711	145.09	1.26	0.609	5.10	6

CONCLUSIONS

The study of the inelastic scattering of alpha particles and the angular correlation between the inelastically scattered alpha particle and the de-excitation gamma ray has been based on the distorted-wave Born approximation theory of inelastic scattering. The nucleus has been treated by using the macroscopic collective model.

In the mass region of tin-120 the optical model is valid and the predicted fits to the elastic scattering data are good. The fits to the data exhibit the usual optical model ambiguities, and these result from the surface reflection type as opposed to volume reflection. The DWBA calculations of the inelastic alpha-particle scattering are of no help in removing these ambiguities. The greater sensitivity of the angular correlation in a DWBA calculation to the optical model parameters also seems to be of no help in removing these ambiguities. The DWBA calculations of the symmetry angles are all similar over a wide range of optical model parameters, and none reproduced the rotations found in the experimental data. Three of the potentials predict a different behavior of the symmetry angle at approximately an alpha scattering angle of 6^{o}, but it is impossible to obtain experiment data at those alpha scattering angles.

The rotations measured in the symmetry angle show a momentum dependence as do the cross sections. The rotations in the symmetry angle scale approximately as $kr_o \sin \theta/2$. So, if structure exists in the symmetry angle data, it will be compressed to forward angles where it is difficult to make an experimental measurement.

Lewis Research Center,
National Aeronautics and Space Administration,
Cleveland, Ohio, October 1, 1969,
129-02.

REFERENCES

1. Baron, Norton; Leonard, Regis F.; Need, John L.; and Stewart, William M.: Elastic and Inelastic Scattering of 40-MeV Alpha Particles From Even Tin Isotopes. NASA TN D-3067, 1965.
2. Leonard, Regis F.; Stewart, William M.; and Baron, Norton: Elastic and Inelastic Scattering of 42-MeV Alpha Particles From Even Tellurium Isotopes. NASA TN D-3991, 1967.
3. Drisko, R. M.; Satchler, G. R.; and Bassel, R. H.: Ambiguities in the Optical Potential for Strongly Absorbed Projectiles. Phys. Letters, vol. 5, no. 5, Aug. 1, 1963, pp. 347-350.
4. Baron, Norton; and Kaminski, Gerald A.: Manufacture of Lithium-Drifted Silicon Surface-Barrier Semiconductor Counters. NASA TN D-3554, 1966.
5. Stewart, William M.; Baron, Norton; Braley, Richard C.; and Leonard, Regis F.: Alpha-Gamma Angular Correlations in the Reaction Carbon 12($\alpha, \alpha'\gamma_{4.433\ MeV}$). NASA TN D-5568, 1969.
6. Banerjee, Manoj K.; and Levinson, Carl A.: Direct Interaction Theory of Inelastic Scattering. Part II. Angular Correlation of Gamma Rays Following Inelastic Scattering. Ann. Phys. (N.Y.), vol. 2, no. 5, Nov. 1957, pp. 499-524.
7. Leonard, Regis F.; Stewart, William M.; Baron, Norton; and Braley, Richard C.: Gamma Ray Angular Correlations Following Inelastic Scattering of 42-MeV Alpha Particles from Magnesium 24. NASA TN D-4683, 1968.
8. Rose, M. E.: The Analysis of Angular Correlation and Angular Distribution Data. Phys. Rev., vol. 91, no. 3, Aug. 1, 1953, pp. 610-615.

9. Blair, John S.: Inelastic Diffraction Scattering. Phys. Rev., vol. 115, no. 4, Aug. 15, 1959, pp. 928-938.

10. Blair, J. S.; and Wilets, L.: Gamma-Ray Correlation Function in the Adiabatic Approximation. Phys. Rev., vol. 121, no. 5, Mar. 1, 1961, pp. 1493-1499.

11. Austern, N.; Butler, S. T.; and McManus, H.: Angular Distributions from (n, p) Nuclear Reactions. Phys. Rev., vol. 92, no. 2, Oct. 15, 1953, pp. 350-354.

12. Satchler, G. R.: Gamma Radiation Following the Surface Scattering of Nucleons. Proc. Phys. Soc., vol. A68, pt. 11, Nov. 1955, pp. 1037-1040.

13. Tobocman, W.: Theory of the (d, p) Reaction. Phys. Rev., vol. 94, no. 6, June 15, 1954, pp. 1655-1663.

14. Broek, H. W.; Yntema, J. L.; Buck, B.; and Satchler, G. R.: Wide-Angle Scattering of 43 MeV Alpha Particles by ^{58}Ni. Nucl. Phys., vol. 64, no. 2, 1965, pp. 259-272.

15. Tobocman, W.: Theory of Direct Nuclear Reactions. Oxford Univ. Press, 1961.

16. Gibbs, W. R.; et al.: Direct Reaction Calculation. NASA TN D-2170, 1964.

17. Baron, Norton; Leonard, Regis F.; and Stewart, William M.: Alpha-Gamma Angular Correlations in the Reaction Nickel 58 $(\alpha, \alpha' \gamma_{1.452 \text{ MeV}})$. NASA TN D-5585, 1969.

18. Melkanoff, Michel A.; Nodvik, John S.; Saxon, David S.; and Cantor, David G.: A FORTRAN Program for Elastic Scattering Analyses With the Nuclear Optical Model. Univ. of California Press, 1961.

NASA-Langley, 1969 —— 24 E-5181

NATIONAL AERONAUTICS AND SPACE ADMINISTRATION
WASHINGTON, D. C. 20546

OFFICIAL BUSINESS

FIRST CLASS MAIL

POSTAGE AND FEES PAID
NATIONAL AERONAUTICS AND
SPACE ADMINISTRATION

POSTMASTER: If Undeliverable (Section 158 Postal Manual) Do Not Return

"The aeronautical and space activities of the United States shall be conducted so as to contribute . . . to the expansion of human knowledge of phenomena in the atmosphere and space. The Administration shall provide for the widest practicable and appropriate dissemination of information concerning its activities and the results thereof."

—NATIONAL AERONAUTICS AND SPACE ACT OF 1958

NASA SCIENTIFIC AND TECHNICAL PUBLICATIONS

TECHNICAL REPORTS: Scientific and technical information considered important, complete, and a lasting contribution to existing knowledge.

TECHNICAL NOTES: Information less broad in scope but nevertheless of importance as a contribution to existing knowledge.

TECHNICAL MEMORANDUMS: Information receiving limited distribution because of preliminary data, security classification, or other reasons.

CONTRACTOR REPORTS: Scientific and technical information generated under a NASA contract or grant and considered an important contribution to existing knowledge.

TECHNICAL TRANSLATIONS: Information published in a foreign language considered to merit NASA distribution in English.

SPECIAL PUBLICATIONS: Information derived from or of value to NASA activities. Publications include conference proceedings, monographs, data compilations, handbooks, sourcebooks, and special bibliographies.

TECHNOLOGY UTILIZATION PUBLICATIONS: Information on technology used by NASA that may be of particular interest in commercial and other non-aerospace applications. Publications include Tech Briefs, Technology Utilization Reports and Notes, and Technology Surveys.

Details on the availability of these publications may be obtained from:

SCIENTIFIC AND TECHNICAL INFORMATION DIVISION

NATIONAL AERONAUTICS AND SPACE ADMINISTRATION

Washington, D.C. 20546